PNAS RESEARCH ARTICLE | IMMUNOLOGY AND INFLAMMATION OPEN ACCESS

Mitochondria regulate MR1 protein expression and produce self-metabolites that activate MR1-restricted T cells

Gennaro Prota[a,1,2], Giuliano Berloffa[a,2], Wael Awad[b,2], Alessandro Vacchini[a], Andrew Chancellor[a], Verena Schaefer[a], Daniel Constantin[a], Dene R. Littler[b], Rodrigo Colombo[a], Vladimir Nosi[a], Lucia Mori[a], Jamie Rossjohn[b,c,1], and Gennaro De Libero[a,1]

Affiliations are included on p. 11.

Edited by Marco Colonna, Washington University in St. Louis School of Medicine, St. Louis, MO; received September 11, 2024; accepted March 11, 2025

Mitochondria coordinate several metabolic pathways, producing metabolites that influence the immune response in various ways. It remains unclear whether mitochondria impact antigen presentation by the MHC-class-I-related antigen-presenting molecule, MR1, which presents small molecules to MR1-restricted T-lymphocytes. Here, we demonstrate that mitochondrial complex III and the enzyme dihydroorotate dehydrogenase are essential for the cell-surface expression of MR1 and for generating uridine- and thymidine-related compounds that bind to MR1 and are produced upon oxidation by reactive oxygen species. One mitochondria-derived immunogenic formylated metabolite we identified is 5-formyl-deoxyuridine (5-FdU). Structural studies indicate that 5-FdU binds in the A'-antigen-binding pocket of MR1, positioning the deoxyribose toward the surface of MR1 for TCR interaction. 5-FdU stimulates specific T cells and detects circulating T cells when loaded onto MR1-tetramers. 5-FdU-reactive cells resemble adaptive T cells and express the phenotypes of naïve, memory, and effector cells, indicating prior in vivo stimulation. These findings suggest that mitochondria may play a role in MR1-mediated immune surveillance.

antigen presentation | MR1 | mitochondria | T cells | formylated metabolite

Significance

Recent reports indicate that T cells can recognize self-metabolites that accumulate in tumor cells and are presented by MHC-related protein 1 (MR1). This study identifies mitochondria as a source of MR1-presented antigens, which are key for promoting MR1 protein expression, generating immunogenic metabolites presented by MR1, and stimulating T cells. The mitochondrial activities involved include complex III, oxidative phosphorylation, the dihydroorotate dehydrogenase enzyme, and de novo pyrimidine synthesis. A nucleobase antigen was identified, specific T cells were isolated, and the MR1-Ag structure was resolved. Therefore, the immunological role of mitochondria extends beyond energy production, highlighting the connection between nucleobase metabolism and immune recognition. This study suggests that tumor cells with unique metabolic alterations are targets for MR1-self-metabolite-specific T cells.

Mitochondria play several essential roles in cellular functions, including energy production, the supply of crucial metabolites, and involvement in processes like cell differentiation, apoptosis, and the cell cycle (1). These activities are carried out through tightly regulated chemical reactions, most notably, oxidative phosphorylation (OXPHOS). The OXPHOS reactions require the operation of four respiratory complexes (CI to CIV), which are crucial for adenosine triphosphate (ATP) production, the synthesis of cellular building blocks, and the generation of reactive oxygen species (ROS) (2). These functions establish mitochondria as central hubs for cellular biochemistry (3).

Mitochondria may also influence the behavior of immune cells. This role has been widely studied, particularly regarding how the tricarboxylic acid (TCA) cycle and energy production affect the differentiation, activation, and proliferation of both innate and adaptive immune cells (4).

Moreover, significant research has highlighted the pivotal role of mitochondrial DNA (mtDNA) in activating innate immune responses (5). Recently, additional functions of OXPHOS in T cell recognition have been suggested. Specifically, decreased OXPHOS activity has been associated with enhanced recognition of cancer cells by T cell receptor (TCR)γδ cells (6), and reduced activity of complex II (CII) in tumor cells has been linked to increased Major Histocompatibility molecule (MHC) class I antigen presentation (7).

The extent to which antigens (Ags) produced by mitochondria can stimulate T cells remains an open question. HLA and CD1 molecules can present peptides or lipids of either mitochondrial origin or those that have been delivered to mitochondria (8–16). These findings suggest that molecules generated within or trafficked through mitochondria can reach cellular compartments where antigen-presenting molecules bind antigens. Mitochondria are a crucial source of metabolites, and changes in mitochondrial activity can significantly alter the cell's metabolome (17, 18). This metabolic role raises the possibility that mitochondria also serve as reservoirs of metabolites that act as antigens capable of stimulating T cells.

The recognition of small molecule metabolites by αβ T cells has been highlighted by discovering the role of the MHC class I-related molecule MR1. MR1 presents a variety of bacterial metabolites to mucosal-associated invariant T (MAIT) cells (19, 20), including 6-formyl pterin (6-FP), a photodegradation product of exogenous folic acid (21), as well as several drugs, drug-like molecules, and dietary antigens (22, 23). MR1 also presents self-antigens to MR1-restricted T (MR1T) cells (24–26) and a population of self-reactive

This article is a PNAS Direct Submission.

[1]To whom correspondence may be addressed. Email: gennaro.prota86@gmail.com, jamie.rossjohn@monash.edu, or gennaro.delibero@unibas.ch.

[2]G.P., G.B., and W.A. contributed equally to this work.

This article contains supporting information online at https://www.pnas.org/lookup/suppl/doi:10.1073/pnas.2418525122/-/DCSupplemental.

Published May 12, 2025.

MAIT cells (27). Given these findings, we hypothesized that MR1 is an ideal candidate for presenting metabolites influenced by mitochondrial activities to various MR1-restricted T cells.

Using pharmacological and genetic approaches to manipulate mitochondrial functions, we found that mitochondria regulate MR1 cell surface expression, contribute to presenting MR1 antigens to T cells, and generate MR1-restricted antigens. These studies establish a mechanistic link between mitochondrial function and MR1-restricted T cell immunity.

Results

Mitochondrial OXPHOS Participates in MR1 Cell Surface Expression. The electron transport chain (ETC) comprises four multisubunit complexes: complexes I to IV (CI to CIV). Complexes I and II initiate the electron flow, transferring electrons from the TCA cycle and glycolysis to ubiquinone, which then delivers them to complex III (CIII) and finally to oxygen via complex IV (CIV) (Fig. 1*A*). We investigated whether the ETC process influences the surface expression of antigen-presenting molecules, including CD1a, CD1b, CD1c, CD1d, MHC class I, MHC class II, and MR1. To do this, cells were exposed to oligomycin, which inhibits several mitochondrial functions such as ATP synthesis, proton translocation, and oxygen consumption (28). The expression of these antigen-presenting molecules on the cell surface was then measured.

Because these molecules typically have low physiological expression levels, THP-1 cells transfected individually with genes for CD1a, CD1b, CD1c, CD1d, or MR1 were used. The results showed that exposure to nontoxic doses of oligomycin significantly reduced the cell surface expression levels of CD1b, CD1d, and MR1. In contrast, the expression levels of other molecules remained unaffected (Fig. 1*B* and *SI Appendix*, Fig. S1 *A* and *B*). The experiment was repeated using primary cells to provide more natural relevance to our observations. Monocytes were treated overnight with a nontoxic dose of oligomycin, and we then measured the expression of MR1, CD1b, and MHC class I and II molecules. A reduction in MR1 and CD1b molecules was observed, while MHC class I and II molecules remained unchanged, thus confirming the observations made with tumor cell lines that overexpress different antigen-presenting molecules (Fig. 1*C* and *SI Appendix*, Fig. S1 *C* and *D*). Focusing on MR1, we investigated whether the inhibitory effect of oligomycin on MR1 surface expression also occurs in other tumor cell lines. The

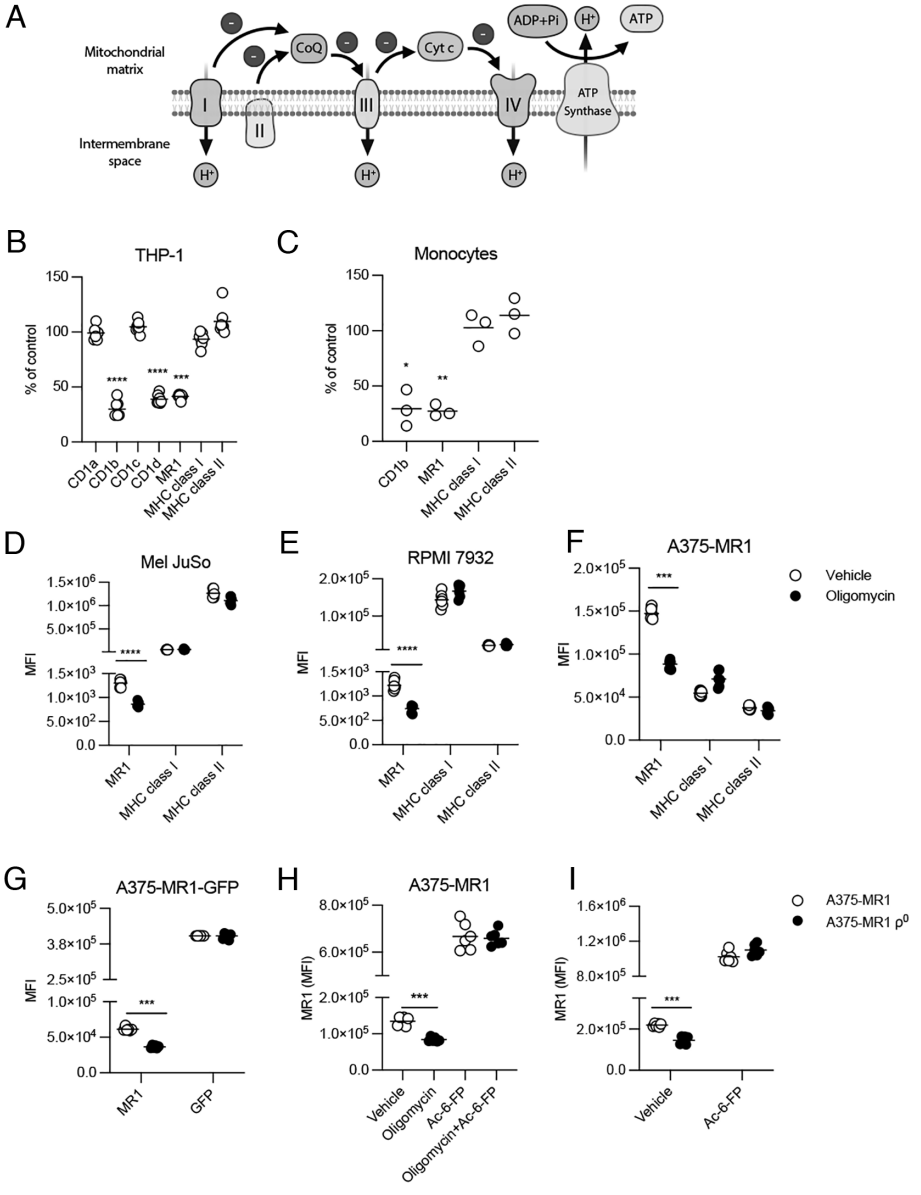

Fig. 1. Blocking of mitochondrial activity reduces MR1 levels on the tumor's cell surface. (*A*) Illustration of mitochondrial ETC composed of four complexes (I-IV). The electron flow is indicated by minus in dark circles and protons by H^+. CoQ, Cytochrome C (Cyt c), and ATP synthase are involved in the process of ATP generation. (*B*) Cell surface expression of antigen-presenting molecules following oligomycin exposure of THP-1 cells (MHC class I and MHC class II) and THP-1 cells individually transfected with CD1a, CD1b, CD1c, CD1d, or MR1. Values represent the percentage of control of n = 7 samples in three independent experiments, and bars represent the mean values. Statistical significance was determined by comparing the control's median fluorescence intensity (MFI) with the MFI of the respective treated group (see below for details). (*C*) Cell surface expression of CD1b, MR1, MHC class I, and MHC class II after oligomycin exposure of freshly isolated monocytes. Values represent the percentage of control from n = 3 samples collected from three healthy donors, and bars indicate the mean values. Statistical significance was assessed by comparing the control's MFI with the MFI of the corresponding treated group (see below for details). (*D*–*F*) Surface expression of MR1, MHC class I, and MHC class II on (*D*) Mel JuSo (n = 6), (*E*) RPMI 7932 (n = 6), and (*F*) A375-MR1 cells (n = 6) treated with oligomycin (closed circles) or vehicle (open circles). (*G*) MR1 and GFP expression levels of A375-MR1-GFP cells after exposure to oligomycin (closed circles) or vehicle (open circles) (n = 6). (*H*) MR1 surface levels of A375-MR1 cells exposed or not to oligomycin or Ac-6-FP or both (n = 6). (*I*) MR1 surface levels of A375-MR1 (open circles) and A375-MR1 ρ^0 cells (closed circles) following or not exposure to Ac-6-FP (20 μM) (n = 6). Statistical evaluation was performed using the Student's *t* test, ****$P \leq 0.001$, ***$P \leq 0.005$, **$P \leq 0.01$, *$P \leq 0.05$. The data show results from two independent experiments out of three performed. See also *SI Appendix*, Figs. S1 and S2.

effect was consistent in Mel JuSo and RPMI 7932 melanoma cell lines, which naturally express detectable levels of MR1, and in A375 melanoma cells transfected with the MR1 gene. In all these cell lines, oligomycin reduced MR1 surface expression without affecting the surface levels of MHC class I and II molecules (Fig. 1 *D*–*F* and *SI Appendix*, Fig. S2*A*).

We used a cell line overexpressing MR1 fused to an enhanced green fluorescent protein (A375-MR1-GFP) to determine whether blocking mitochondrial activity leads to reduced expression of MR1 protein. Although oligomycin reduced MR1 surface expression, it did not affect the overall GFP signal detected by flow cytometry (Fig. 1*G*), and Western blot analysis confirmed that total MR1 protein levels remained similar in both exposed and not exposed cells (*SI Appendix*, Fig. S2*B*).

To explore whether oligomycin exposure results in the accumulation of intracellular, ligand-receptive MR1, we incubated cells with acetyl-6-formyl pterin (Ac-6-FP), a potent MR1 ligand known to stabilize and enhance MR1 surface expression (29). Ac-6-FP induced similar levels of MR1 on the surface of both oligomycin-exposed and unexposed cells, indicating that ligand-receptive MR1 accumulates intracellularly in cells exposed to oligomycin (Fig. 1*H*). These findings suggest that functional mitochondria are crucial for the proper maturation and surface expression of MR1 protein.

We generated A375 cell variants lacking mitochondrial DNA (A375-MR1 ρ^0) to explore mitochondria's role further using established methods (30). These ρ^0 cells are deficient in all mitochondrial-encoded genes and thus cannot assemble functional mitochondrial complexes. Consequently, they lack the central enzymes required for aerobic energy metabolism and rely solely on anaerobic glycolysis for ATP production. Additionally, ρ^0 cells cannot generate mitochondrial ROS and cannot synthesize pyrimidines (31).

Multiple lines of evidence confirmed the deficiency in mitochondrial DNA, including the absence of mitochondrial genes ND-1 and ND-5, significantly reduced mitochondrial membrane potential (MMP), decreased intracellular ROS levels, and reduced mitochondrial mass (*SI Appendix*, Fig. S2 *C* and *G*).

A375-MR1 ρ^0 cells exhibited a reduction in MR1 surface expression. However, incubation with the MR1 ligand Ac-6-FP restored MR1 levels to those observed in wild-type cells (Fig. 1*I*). These findings indicate that mitochondrial OXPHOS is crucial for the maturation of MR1. However, in the presence of ligands like exogenous Ac-6-FP, MR1 can egress from the endoplasmic reticulum (ER) to the cell surface, even in the absence of functional mitochondria.

CIII Activity Is Essential to Maintain Basal Levels of MR1 on the Cell Surface. To investigate the role of electron flow in the maturation of MR1, we analyzed the expression levels of antigen-presenting molecules following the selective inhibition of each mitochondrial complex. This inhibition was achieved using specific inhibitors: rotenone for complex I (CI), 3-nitro propionic acid (3-NPA) for complex II (CII), antimycin A for complex (CIII), and sodium azide (NaN_3) for complex IV (CIV) (7, 32, 33).

The results showed a significant decrease in MR1 surface expression when CIII activity was inhibited by antimycin A. In contrast, inhibition of CI, CII, and CIV did not affect MR1 surface levels (Fig. 2*A* and *SI Appendix*, Fig. S3*A*). Conversely, inhibition of CII, CIII, and CIV led to an increase in the cell surface expression of HLA-I and HLA-DR (Fig. 2 *B* and *C* and *SI Appendix*, Fig. S3*A*). These observations support recent findings in mice that emphasize the role of CII in MHC class I protein expression (7) and extend this knowledge to include CIII and CIV. Additionally, the upregulation of HLA-DR on the cell surface further underscores the impact of these complexes on antigen presentation (Fig. 2*C* and *SI Appendix*, Fig. S3*A*).

To further validate the role of CIII in maintaining MR1 levels on the cell surface, we restored Coenzyme Q (CoQ) oxidase activity in A375-MR1 ρ^0 cells by transducing them with the Alternative Oxidase (AOX) gene from the yeast *Emericella nidulans*. AOX serves as an alternative electron transport pathway in lower eukaryotes and plants. It is well tolerated in cultured higher eukaryotic cells, bypassing CIII, thus restoring electron transport in ρ^0 cells (Fig. 2*D*) (34, 35).

AOX also confers resistance to complexes III (CIII) and IV (CIV) inhibitors, such as cyanide and antimycin A (34, 36). ρ^0 cells, lacking functional mitochondria, are uridine auxotrophs due to the inactivation of dihydroorotate dehydrogenase (DHODH), an enzyme located on the outer surface of the inner mitochondrial membrane and essential for de novo pyrimidine synthesis (37). Expression of AOX in A375-MR1 ρ^0 cells enabled these cells to survive without supplemental uridine (Fig. 2*E*), confirming the functional activity of AOX in these transfected cells.

Restoring electron flow with AOX in A375-MR1 ρ^0 cells led to a significant increase in MR1 surface expression (Fig. 2*F*). When the potent MR1 ligand Ac-6-FP was present, MR1 levels were comparable in both ρ^0 and ρ^0 AOX cells (Fig. 2*F*), indicating that both cell types express functional MR1 proteins capable of binding suitable ligands and being transported to the cell surface. These findings establish a strong link between mitochondrial CIII activity and the regulation of MR1 surface expression.

CIII Inhibition Alters the Stimulation of Some MR1T Cells. The availability of ligands influences the levels of MR1 on the plasma membrane (38). Therefore, the observed low surface expression of MR1 might result from a reduced presence of endogenous ligands of mitochondrial origin or related to mitochondrial activity. Thus, we measured the effects of APCs exposure to drugs inhibiting the activity of different mitochondrial complexes on the stimulation of self-reactive MR1-restricted T cell clones to explore whether CIII activity affects the generation of stimulatory antigens. These assays utilized four MR1-restricted T cell clones: three self-reactive clones (DGB129, TC5A87, and MCA3C3) and one classical MAIT cell clone (MRC25), which responds to the microbial metabolite 5-OP-RU (24, 26, 27). A375-MR1 cells were used as APC after exposure to the CIII inhibitors antimycin A and atovaquone (32, 39). Both treatments impaired the stimulation of the clones DGB129 and TC5A87, while the activation of MCA3C3 and the MAIT clone MRC25 was unaffected (Fig. 3 *A* and *B*). When we stimulated DGB129, TC5A87, and MCA3C3 cells with APC treated with drugs that inhibit each mitochondrial complex, a decreased stimulation was observed only when APCs were exposed to the CIII inhibitor antimycin A (*SI Appendix*, Fig. S3*B*).

To further investigate the effects of CIII inhibition, the responses from a library of eleven MR1T clones were examined (*SI Appendix*, Fig. S3 *C* and *D*). The results identified two distinct groups: seven CIII inhibition-sensitive clones and four CIII inhibition-insensitive clones. The fact that some MR1T clones responded similarly to treated and untreated APCs suggested that CIII inhibition did not universally compromise the antigen presentation capacity of A375-MR1 cells. This was further supported by the observation that APCs exposed to CIII inhibitors could present the 5-OP-RU antigen to the MAIT cell clone MRC25 as effectively as untreated APCs (Fig. 3*B*). These findings indicate that CIII activity is crucial for generating or presenting a group of endogenous antigens.

A functional CIII maintains the CoenzymeQ (CoQ) pool, necessary for DHODH activity. This enzyme is critical for the de

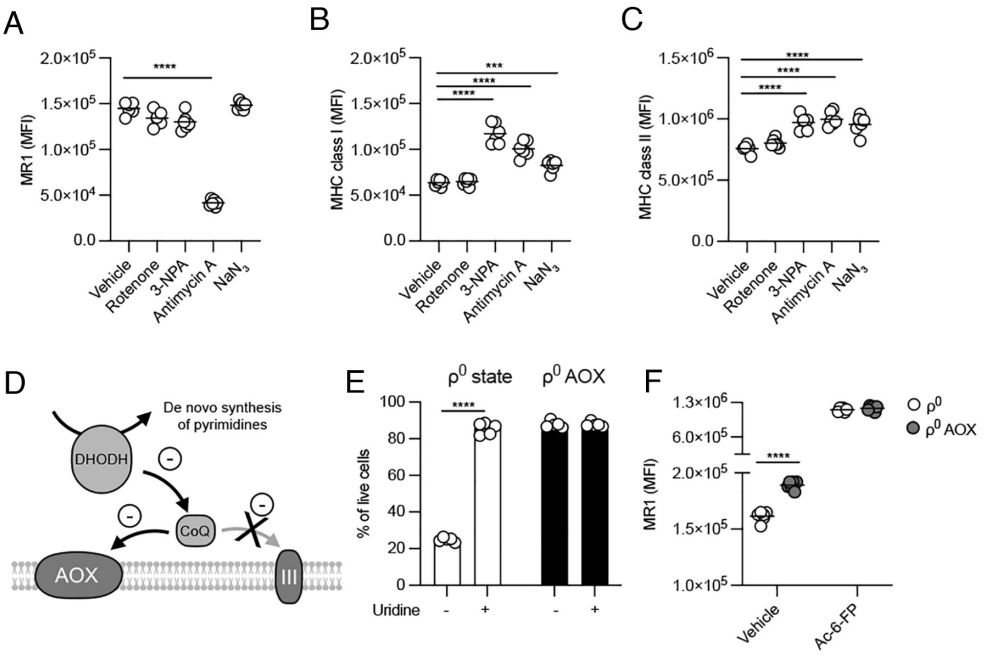

Fig. 2. CIII activity is essential to maintain basal levels of MR1 on the cell surface. (*A*–*C*) Cell surface expression of (*A*) MR1, (*B*) MHC class I, and (*C*) MHC class II molecules following exposure of A375-MR1 cells to rotenone, 3-NPA, antimycin A, or NaN_3. Values represent the MFI of n = 6 samples, and bars represent the mean values. (*D*) Illustration showing the reactivation of de novo synthesis of pyrimidines in ρ^0 cells expressing AOX. In ρ^0 cells, CIII cannot accept electrons (minus in circles) from CoQ because it is not functional. After the AOX gene transfer, CoQ donates electrons to AOX, thus becoming substrate available for DHODH, which becomes functional. (*E*) Survival of A375-MR1 ρ^0 cells (open columns) or AOX-expressing A375-MR1 ρ^0 cells (filled columns) after incubation in a medium containing dialyzed fetal bovine serum with or without uridine. The percentage of viable cells is shown (n = 5). (*F*) MR1 levels of A375-MR1 ρ^0, or A375-MR1 ρ^0 AOX assessed by flow cytometry after overnight incubation with Ac-6-FP (20 μM) or vehicle. MFI is shown (n = 6). Statistical evaluation was performed using the one-way ANOVA with Tukey's test, ****$P \le 0.001$, ***$P \le 0.005$, (*A*–*C*), or the Student's *t* test, ****$P \le 0.001$ (*E* and *F*). The data shown are from two independent experiments out of three performed. See also *SI Appendix*, Fig. S3.

novo synthesis of pyrimidines (Fig. 4*A*) (40), previously shown to form MR1 ligands (20, 23, 41). We explored whether mitochondrial regulation of MR1T cell stimulation relies on CIII regulation of DHODH generation of uridine-based antigens. To test this, APCs were sequentially inhibited in their CIII activity, supplemented with uridine (that feeds the de novo synthesis of pyrimidines overcoming DHODH inactivity), and assessed for their ability to stimulate MR1T cells. The results showed that APCs exposed to CIII inhibitors lost their ability to stimulate the CIII-dependent MR1T cell clones DGB129 and TC5A87. However, adding uridine fully reverses this inhibition (Fig. 3*C*). In contrast, APCs continued to stimulate the CIII-independent MCA3C3 clone regardless of uridine addition (Fig. 3*C*).

These findings suggest that uridine supplementation can overcome the effects of CIII inhibition, indicating that APCs generate uridine-dependent compounds recognized by specific self-reactive MR1T cells. However, these uridine-dependent antigens do not appear to be involved in stimulating microbial-reactive MAIT cells. This supports the hypothesis that CIII-dependent pathways contribute specifically to generating endogenous ligands that activate a population of MR1-restricted T cells.

Uridine-Dependent Compounds Rescue MR1T Cell Stimulation in DHODH-Deficient APCs. To further investigate the nature of the uridine-dependent MR1T cell antigens, we exposed APCs to brequinar, a well-characterized DHODH inhibitor (42). The doses of brequinar were nontoxic and did not affect antigen presentation to MAIT cells (*SI Appendix*, Fig. S4*A*). Subsequently, we assessed the stimulation of MR1T cells in the presence or absence of exogenous uridine. Brequinar-treated cells had a significantly reduced capacity to stimulate the MR1T cell clones DGB129 and TC5A87. We also included two additional CIII-dependent MR1T clones, GP2A36 and GP2A20, which similarly exhibited reduced responses when exposed to brequinar-treated cells, except in the presence of uridine (Fig. 4*B*). In contrast, the response of the CIII-independent MR1T clone MCA3C3 remained unaffected (Fig. 4*B*).

These findings mirrored the results obtained with CIII inhibitors, suggesting that the inhibition of DHODH impairs the generation of uridine-dependent antigens necessary for activating specific MR1T cells. To confirm these observations, we generated DHODH-deficient (DHODH-KO) cells (*SI Appendix*, Fig. S4*B*). The absence of DHODH was verified through Western blot analysis (*SI Appendix*, Fig. S4*B*). The DHODH-KO cells failed to stimulate the DGB129 and TC5A87 clones efficiently, and uridine supplementation significantly enhanced their response (*SI Appendix*, Fig. S4 *C* and *D*). Consistent with previous findings, the DHODH-KO cells effectively stimulated the CIII-independent MCA3C3 clone, and uridine addition did not alter this response (*SI Appendix*, Fig. S4 *C* and *D*).

These experiments confirmed that DHODH activity is crucial for the generation of specific uridine-dependent antigens that activate certain MR1T cells, further underscoring the role of mitochondrial function, particularly CIII and DHODH, in shaping the repertoire of MR1-restricted antigens.

To identify which compounds downstream of DHODH could restore the stimulation of CIII-dependent MR1-restricted T (MR1T) cell clones, we focused on intermediates in the de novo pyrimidine synthesis pathway. DHODH is the fourth enzyme in this pathway, and its immediate downstream products include uridine monophosphate (UMP), uridine diphosphate (UDP), and uridine triphosphate (UTP) (40) (Fig. 4*A*).

Supplementing DHODH-deficient (DHODH-KO) cells with UTP fully restored their ability to stimulate MR1T cell clones, indicating that UTP can compensate for the loss of DHODH activity (*SI Appendix*, Fig. S4*D*). In contrast, cytidine triphosphate

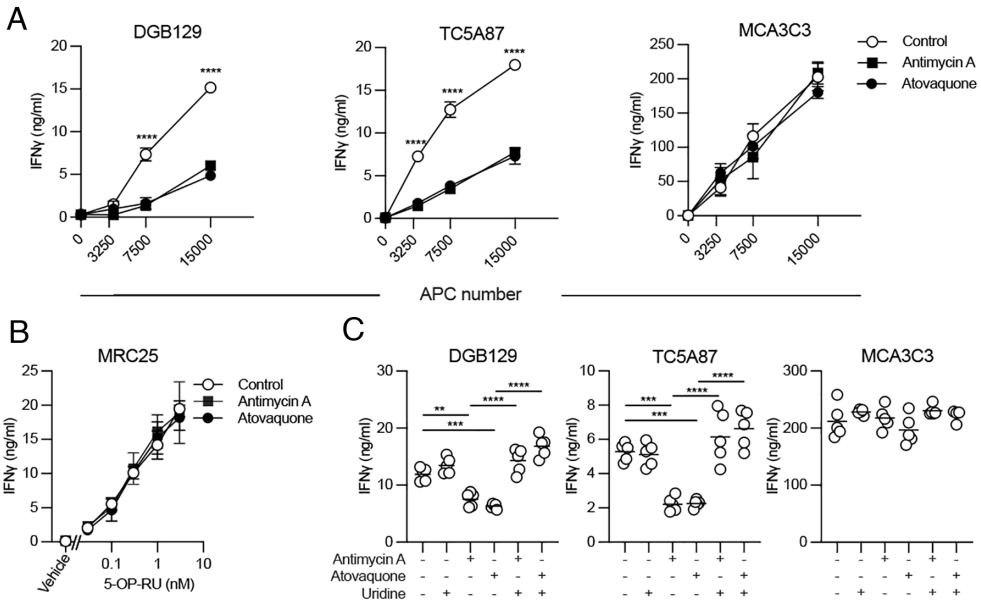

Fig. 3. CIII inhibition decreases the response of some MR1T cell clones. (*A*) Response of the indicated MR1T cell clones to increasing numbers of A375-MR1 cells (APC number per well) exposed to antimycin A (filled squares) or atovaquone (filled circles) compared to unexposed cells (open circles). The released IFNγ is shown as the mean of triplicates ± SD after overnight incubation. Data are from one experiment representative of three independently performed experiments. (*B*) Response of the MAIT clone MRC25 to increasing doses of 5-OP-RU presented by A375-MR1 cells exposed to antimycin A (filled squares) or atovaquone (filled circles) or unexposed (open circles). The released IFNγ is shown as the mean of triplicates ± SD. Data are from one experiment representative of three independently performed experiments. (*C*) Response of the indicated MR1T cell clones to A375-MR1 cells exposed to antimycin A or atovaquone in the presence or absence of uridine. The released IFNγ is shown for each sample. Bars indicate the mean values (n = 5). The data displayed are from two independent experiments out of three performed. One-way ANOVA with Tukey's test, ****$P \le 0.001$, ***$P \le 0.005$, **$P \le 0.01$. See also *SI Appendix*, Fig. S3.

(CTP) did not restore MR1T cell stimulation (*SI Appendix*, Fig. S4*D*), suggesting that uridine-dependent compounds, rather than cytidine-dependent ones, are crucial for this activity.

To further validate these results, we repeated the rescue experiments using APCs treated with brequinar and supplemented with UMP, UDP, UTP, and CTP. Similar to the findings with DHODH-KO cells, UMP, UDP, and UTP effectively restored the stimulation of MR1T cell clones, while CTP did not (Fig. 4*C*), thus reinforcing the possibility that uridine-dependent compounds are critical for activating MR1T cells.

Additionally, we tested thymidine, a product of deoxy-UMP conversion, to see whether it could also restore MR1T cell stimulation. Thymidine fully recovered the activation of MR1T cell clones GP2A36 and GP2A20 while only partially restoring the activation of DGB129 and TC5A87 cells (Fig. 4*C*). These results indicate that while uridine is essential for stimulating all tested CIII-sensitive MR1T cells, thymidine only partially rescues the activation of specific MR1T clones. In summary, these experiments highlight that among the CIII-sensitive MR1T cells, uridine and its downstream products are critical for their activation. In contrast, thymidine only partially rescues some MR1T cell clones' reactivity.

We also checked whether uridine, UMP, UDP, UTP, and thymidine act as MR1T cell antigens. None of these compounds increased MR1 surface expression on APCs (*SI Appendix*, Fig. S5*A*), nor did they stimulate MR1T cells when added directly to fixed APCs (*SI Appendix*, Fig. S5*B*). These findings suggested that the compounds' rescue effects are related to their intracellular modification rather than their direct binding to MR1.

Given that mitochondria are key producers of ROS, which can cause DNA damage, nucleoside, and nucleotide oxidation (43, 44), we explored whether ROS play a role in the antigenicity of the compounds. Physiological levels of ROS can oxidize methyl groups in pyrimidines (45). Since the MR1T cell clones GP2A36 and GP2A20 responded to thymidine, we hypothesized that scavenging intracellular ROS might affect their responsiveness. We tested this hypothesis by testing the ROS scavenger N-acetylcysteine (NAC) (46).

Exposure to NAC reduced the reactivity of all tested MR1T cells to varying degrees (Fig. 4*D*), indicating ROS are involved in generating stimulatory antigens. Significantly, NAC completely inhibited the rescue effect of thymidine on GP2A36 and GP2A20 clones, demonstrating that ROS are essential for this response (Fig. 4*D*). In contrast, NAC minimally impacted DGB129 and TC5A87 reactivities, which were less affected by thymidine, reinforcing that ROS and thymidine are crucial for activating a subset of MR1T cells that recognize thymidine nucleobase adducts.

These results suggest that MR1T cells exhibit different sensitivities to uridine, thymidine, and ROS, highlighting the role of the nonenzymatic ROS-mediated oxidation of nucleobases and the interplay between these compounds in antigen generation.

5-Formyl-Deoxyuridine Is an MR1T Cell Antigen. The involvement of ROS and thymidine in stimulating specific MR1T cell clones led us to investigate their potential connection. We focused on 5-formyl-deoxyuridine (5-FdU), a modified nucleoside formed by oxidative damage to thymidine, which is generated in a ROS-dependent but enzyme-independent manner (45, 47, 48). Our findings that thymidine and ROS are required to restore MR1T cell stimulation suggested that 5-FdU might play a role as a stimulating metabolite. To explore this, we tested whether 5-FdU and 5-formyl uracil (5-FU)—a derivative of 5-FdU without the ribose moiety (Fig. 5*A*)—could bind MR1. Both 5-FdU and 5-FU efficiently competed with 5-OP-RU and inhibited MAIT cell stimulation, indicating that these compounds bind MR1 but do not stimulate MAIT cells (Fig. 5*B*).

We then assessed the antigenicity of 5-FdU and 5-FU by evaluating the responses of the GP2A20 and GP2A36 clones, which previously showed sensitivity to thymidine and ROS. Both GP2A20 and GP2A36 clones responded to fixed APCs treated

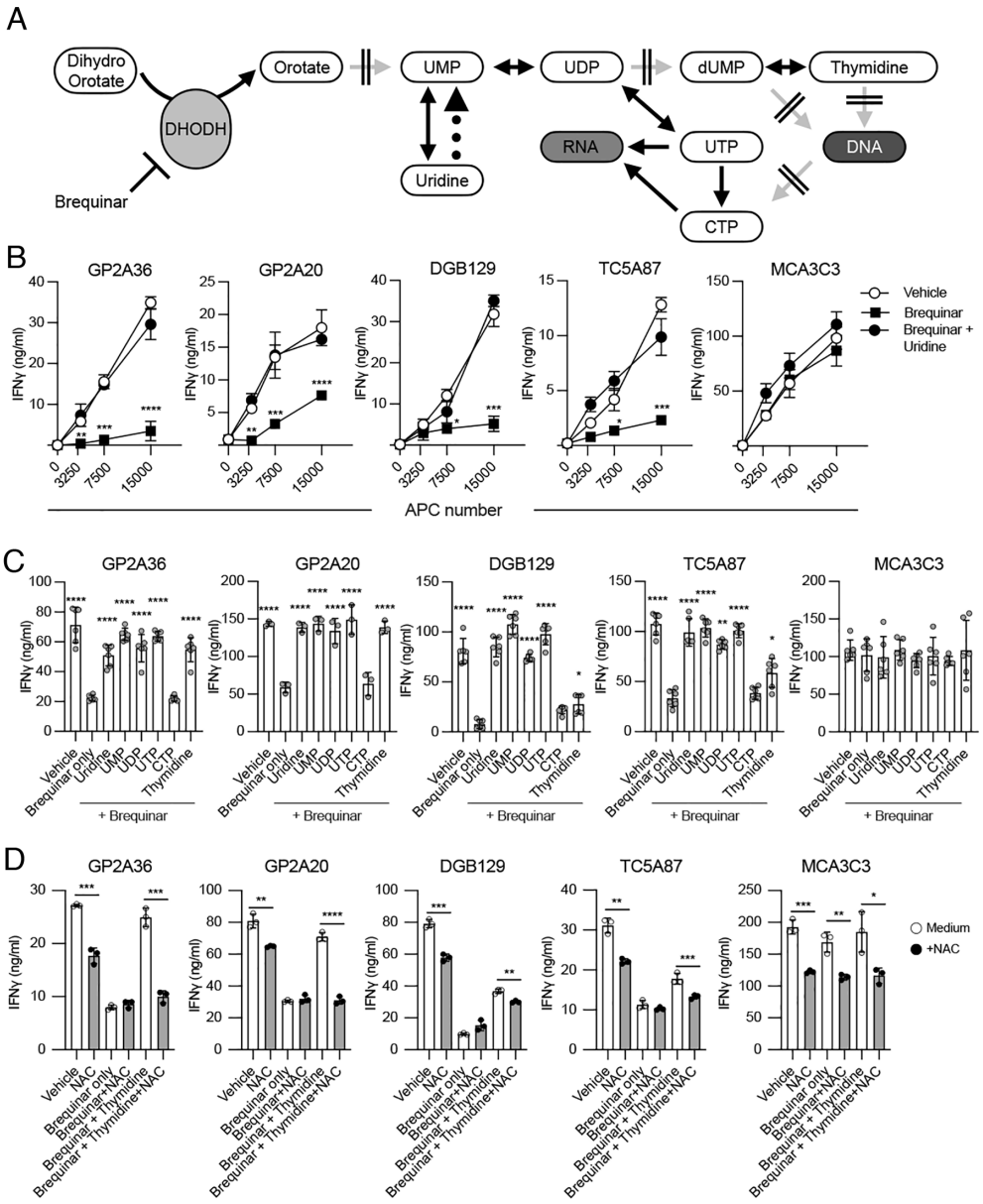

Fig. 4. Uridine derivatives rescue MR1T cell recognition of DHODH-inhibited cells. (*A*) Schematic representation of the de novo pyrimidine synthesis pathways downstream of DHODH. This enzyme catalyzes the fourth enzymatic step, the ubiquinone-mediated oxidation of dihydroorotate to orotate. Interrupted gray arrows indicate that intermediates exist between the specified compounds. The dotted arrow shows that uridine can also serve as a precursor of UMP through uridine kinase, independent of DHODH. (*B*) Response of five MR1T cell clones to various numbers of A375-MR1 cells (APC number per well) exposed to brequinar (filled squares), brequinar + uridine (filled circles), or vehicle (open circles). Data are from one experiment representative of three independently performed experiments. (*C*) Response of the same MR1T cell clones as in (*B*) to A375-MR1 cells exposed to brequinar and the indicated nucleosides or nucleotides. The released IFNγ is the mean ± SD (n = 6). The statistical significance refers to comparison with the group "Brequinar only." The data displayed is from two independent experiments out of three performed. (*D*) Response of the CIII-dependent MR1T cell clones as in (*B*) after exposure to brequinar only, brequinar + thymidine, with or without NAC. Values indicate the mean ± SD of triplicates. Data are from one experiment representative of three independently performed experiments. One-way ANOVA with Tukey's test, ****$P \le 0.001$, ***$P \le 0.005$, **$P \le 0.01$, *$P \le 0.05$. See also *SI Appendix*, Figs. S4 and S5.

with 5-FdU but not to 5-FU, indicating that Ag-processing is not required. Neither clone reacted to Ac-6-FP or 5-OP-RU, which served as negative controls (Fig. 5*C*). In contrast, the MAIT MRC25 clone responded exclusively to 5-OP-RU (Fig. 5*C*). Additionally, the DGB129, TC5A87, and MCA3C3 clones did not respond to either 5-FdU or 5-FU (*SI Appendix*, Fig. S5*C*). These findings together indicated that 5-FdU is an antigenic metabolite recognized by specific MR1T cell clones in a manner dependent on both ROS and thymidine, further elucidating the complex interaction between mitochondrial activity, metabolite generation, and T cell stimulation.

To confirm the antigenicity of both uridine derivatives, we tested the response of GP2A20 and GP2A36 cells to plastic-bound MR1 previously refolded in the presence of 5-FdU or 5-FU. Both clones reacted only to the MR1-5-FdU complexes, and their response was fully inhibited by anti-MR1 mAbs (Fig. 5*D*). Also, in this assay, DGB129, TC5A87, and MCA3C3 cells did not react to MR1-5-FdU complexes (*SI Appendix*, Fig. S5*D*).

To assess whether this interaction is TCR-dependent, Jurkat (JK) cells expressing the GP2A36 (JK-GP2A36) and the GP2A20 (JK-GP2A20) TCRs were stained with four tetramers loaded with 5-FdU, 5-FU, 5-OP-RU, or Ac-6-FP. Control JK cells expressing the MAIT MRC25 TCR were stained only by the MR1-5-OP-RU tetramer, and none of the MR1 tetramers stained the JK cells expressing the DGB129 TCR (Fig. 5*E*). JK cells expressing the E8 TCR that binds MR1 independently from the bound antigen

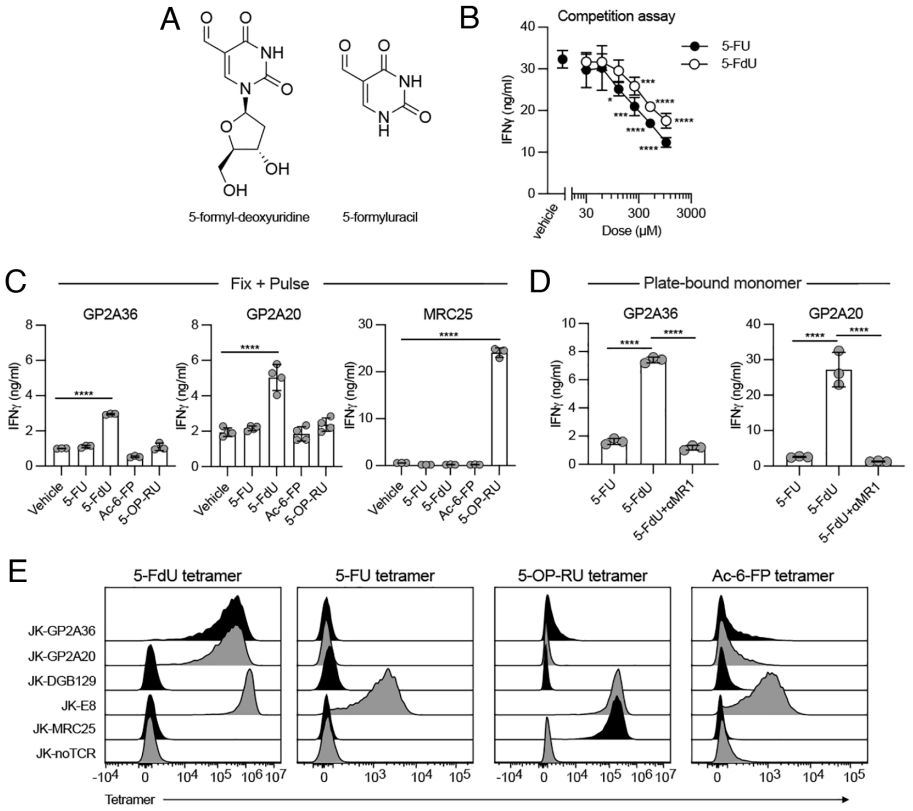

Fig. 5. 5-FdU stimulates MR1T cell cells. (*A*) Structure of 5-formyl-deoxyuridine and 5-formyl-uracil. (*B*) Competition for MR1 binding of 5-FdU or 5-FU assessed by the response of the MRC25 MAIT cell clone to 5-OP-RU presented by fixed A375-MR1 cells pulsed with increasing concentrations of 5-FdU or 5-FU. The released IFNγ is shown as the mean of triplicates ± SD. (*C*) Response of two MR1T and control MAIT clones to A375-MR1 fixed and then pulsed with the indicated antigens. The released IFNγ is shown as the mean of triplicates ± SD. (*D*) Response of the indicated MR1T cell clones to plastic-bound sMR1 monomers refolded with 5-FdU in the presence or absence of anti-MR1 mAbs. The released IFNγ is shown as the mean of triplicates ± SD. (*E*) Staining of JK cells transduced with the indicated TCR genes and stained with various PE-labeled MR1-tetramers. Data are from one experiment representative of three independently performed experiments. One-way ANOVA with Tukey's test, ****$P \le 0.001$, ***$P \le 0.005$, *$P \le 0.05$. See also *SI Appendix*, Fig. S5.

(27) were used here as a positive control of the refolded tetramers. As expected, they were stained with all tetramers (Fig. 5*E*). JK-GP2A36 and JK-GP2A20 were stained with the 5-FdU tetramer only, confirming the specific binding of those TCRs (Fig. 5*E*). Thus, 5-FdU acts as an antigen for specific MR1T cells, and the ribose moiety of the molecule is critical for recognition by the tested MR1T cells.

MR1-5-FdU Tetramer-Positive (tetP) T Cells Are Present in Healthy Donors and Are Phenotypically Diverse. Having identified 5-FdU as a specific antigen for MR1-restricted T cells, we assessed the ex vivo frequency of MR1-5-FdU-reactive T cells in healthy individuals using multicolor flow cytometry. To ensure accurate identification of binding cells, a stringent gating strategy was employed to select events that were only double-positive for MR1-5-FdU-PE and MR1-5-FdU-APC tetramers (*SI Appendix*, Fig. S6 *A* and *B*).

The analysis revealed that MR1-5-FdU tetP T cells were present at very low frequencies, ranging from 0.002 to 0.008% of the total T cells, with a median frequency of 0.003% (Fig. 6*A* and *SI Appendix*, Fig. S7*A*). Notably, about 15% of these tetP cells also bound to the MR1-6-FP tetramer, indicating cross-reactivity with another MR1 ligand. However, these cells very rarely bound to the MR1-5-OP-RU tetramer, suggesting no unspecific binding of MR1 itself (Fig. 6*B* and *SI Appendix*, Fig. S7*A*).

The MR1-5-FdU-reactive T cells exhibited significant interindividual variability in both frequency and phenotype. Flow cytometric analysis revealed that these cells were distributed across several subsets based on CCR7 and CD45RA expression. Specifically, the MR1-5-FdU-reactive T cells included naïve-like T cells (T_N, median 56%), central memory-like (T_{CM}, median 4.7%), effector memory-like (T_{EM}, median 19%), and terminally differentiated effector memory-like (T_{EMRA}, median 10%) T cells (Fig. 6*C* and *SI Appendix*, Fig. S7*B*). These findings indicate that MR1-5-FdU-reactive T cells are diverse, encompassing both naïve and antigen-experienced T cell subsets, reflecting a broad range of developmental and activation states.

To further elucidate the characteristics of MR1-5-FdU-reactive T cells, we performed a cluster analysis comparing MR1-5-FdU tetP and tetramer-negative (tetN) populations based on the expression of 10 surface markers analyzed by spectral flow cytometry. This analysis aimed to identify distinct subpopulations enriched or depleted within the MR1-5-FdU tetP cells (Fig. 6 *D*–*F*). Fourteen populations were identified (6 $CD4^+$, 6 $CD8^+$, and 2 DN). Within the MR1-5-FdU tetP cells, cluster 4 was significantly enriched. In contrast, clusters 9 and 12 were depleted (Fig. 6*F*). Cluster 4 was the most abundant $CD8^+$ cluster and was composed of naïve-like cells ($CCR7^+$ $CD45RA^+$). In contrast, both depleted clusters comprised $CD4^+$ effector memory-like cells ($CCR7^-$ $CD45RA^-$), one expressing CD39, the other KLRG1 markers. Cluster 13 represented minimal cells expressing MAIT cell markers such as CD161, CCR5, and KLRG1. These cells stained very weakly with MR1-5-OP-RU tetramers, suggesting they might be MAIT cells with weakly cross-reactive TCRs, consistent with previous findings (27). These data indicate that MR1-5-FdU tetP cells are present within healthy donors and phenotypically similar to adaptive T cells.

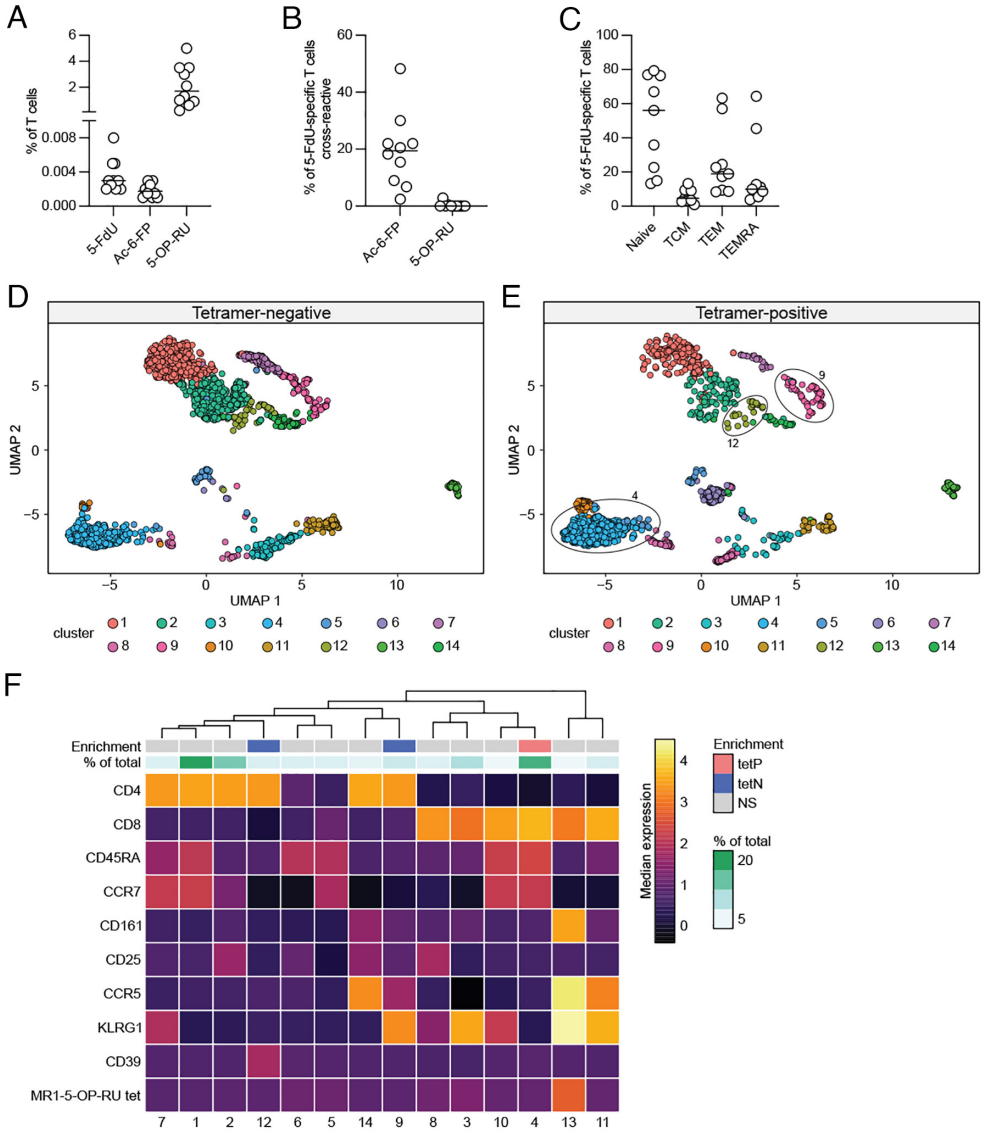

Fig. 6. Ex vivo analysis of MR1-5-FdU tetP cells. (*A*) Ex vivo frequencies of MR1-5-FdU tetP T cells from the peripheral blood of 10 healthy donors. Dots represent individual donors; the horizontal bars represent the median values. (*B*) Ex vivo frequencies of MR1-5-FdU tetP T cells that costain with the MR1-6-FP tetramer or the MR1-5-OP-RU tetramer. Dots represent individual donors; the horizontal bars represent the median values. (*C*) Percentages of naïve, central memory (T_{CM}), effector memory (T_{EM}), and terminally differentiated (T_{EMRA}) T cell populations within the MR1-5-FdU tetP T cells. Dots represent individual donors; the horizontal bars represent the median values. (*D* and *E*) Uniform Manifold Approximation and Projection of the cells were used for the clustering analysis, with cluster identity overlaid as color on tetN (*D*) or tetP (*E*) cells. The cells within clusters 4, 9, and 12 are circled. (*F*) Heatmap of median asinh-transformed expression of the markers used for clustering. Color scales indicate the enrichment of MR1-5-FdU tetP cells and tetN cells and the fraction of total cells (% of total) in each cluster. See also *SI Appendix*, Figs. S6 and S7.

Crystal Structures of MR1-5FU and 5-FdU Complexes. Next, we solved the structures of MR1 presenting 5-FdU and 5-FU. We used the A-F7 TCR as a crystallization aid to achieve this, as MR1 binary complexes have generally been more challenging to crystallize. The crystal complexes diffracted to ~2.2 Å resolution (*SI Appendix*, Table S1 and Fig. 7), exhibiting unambiguous electron densities for the ligands within the MR1 antigen-binding pocket (Fig. 7 *A* and *B*). Analysis of the MR1 binding cleft from the solved structures revealed that the two metabolites were located within the A'-pocket of the MR1 antigen-binding cleft and formed a Schiff base bond with MR1-Lys43 (Fig. 7 *C* and *D*). Despite the chemical differences between these nucleobases, minimal conformational changes within the A'-pocket residues were observed, and the side chains of most MR1 ligand-binding residues were largely conserved (Fig. 7 *E*–*G* and *SI Appendix*, Fig. S8).

In both structures, the two ligands interact predominantly with the MR1 α1-domain (Fig. 7 *F* and *G*). The MR1-Lys43 side chain displacement is apparent when comparing both models with the MR1-5-OP-RU model (Fig. 7 *E*–*G*). The pyrimidine rings of both nucleobases were stabilized by a network of H-bonds with Arg9 and Ser24 of MR1, along with van der Waals interactions with Tyr7, Leu66, and Trp69 of MR1 (Fig. 7 *F* and *G*). These observations confirm previous findings on the essential roles of MR1-Lys43 and Arg9 in stabilizing the Ag binding within the MR1 cleft (49). Furthermore, the deoxyribose sugar of 5-FdU is leaning toward the narrow outer side of the A'-pocket in a different orientation than that of the ribityl chain of 5-OP-RU (Fig. 7*B*). Here, two conformations of the deoxyribose sugar were observed in the pocket with the sugar moiety sandwiched between the MR1-Trp156 and Trp164 of the α2 helix residues and the MR1-Tyr62 of the α1 helix, forming a network of polar and van

der Waals interactions (Fig. 7*G*). Neither ligand stimulated MAIT cells, attributable to a lack of favorable contact with the MAIT TCR (*SI Appendix*, Fig. S8). However, unlike 5-FU, which is closely sequestered within the A'-pocket of MR1, the deoxyribose sugar of 5-FdU is solvent-exposed and thus represents a potential TCR contact point for MR1-restricted TCRs that are reactive to this ligand.

Discussion

These findings attribute two functions to mitochondria relevant to T cell–mediated immunity. The first is that mitochondrial activity is necessary to maintain physiological levels of the antigen-presenting molecule MR1 on the plasma membrane. Without mitochondrial genes, MR1 protein accumulates in the ER and remains available for ligand binding, likely explained by the reduced MR1 antigen content since Ac-6-FP rescues surface expression.

MR1 protein expression is subject to a unique type of regulation that still needs to be fully understood. Our findings indicate that mitochondria-dependent uridine-related compounds contribute to MR1 protein expression on the cell surface, probably by stabilization of the nascent protein, mimicking peptides binding with high affinity to MHC class I molecules that promote their maturation (50). MR1 can also be forced to remain in the ER, as occurs with a synthetic uracil derivative (23). Whether molecules with such inhibitory properties are naturally present in the cell is yet to be determined. If this were the case, mitochondria might contribute to the balance between two types of molecules that either block or promote MR1 egression from ER. A relatively high abundance of compounds that promote egression would increase cell surface MR1, thus facilitating the presentation of endogenous and microbial high-affinity ligands.

A second main finding of this study is that pyrimidine adducts derived from self can form stable complexes with MR1 and stimulate specific MR1T cells. These molecules represent a class of endogenous antigens that stimulate self-reactive MR1T cells. These MR1-restricted endogenous antigens add to and differ from the recently identified nucleobase adducts derived from the condensation of carbonyls with purines and pyrimidines (26, 51) and the binding of a bile acid-derived compound (25). Among the carbonyl adducts of nucleobases, mitochondria promote their formation by two independent mechanisms, i.e., by i) generating pyrimidine bases and ii) accumulation of ROS, which contribute directly to pyrimidine oxidation (45, 47, 48), activation of pro-tumor signaling and metabolic reprogramming (52) and carbonyl generation (53, 54). The accumulation of carbonyl adducts increases in tumor cells (55, 56), which could explain the observed preferential MR1T response to tumor cells (26, 51).

The data also revealed the existence of different populations of MR1T cells according to the type of antigen specificity. The first is not sensitive to the inhibition of CIII. In contrast, the second and third populations are CIII-sensitive but differ in antigen specificity, as indicated by differential reactivity to uridine- and thymidine-dependent molecules. Thus, mitochondria may give rise to various antigens stimulating different MR1T cells.

Among the thymidine-dependent antigens, 5-FdU stimulated some MR1T cells. This adduct has been described within cells as a consequence of oxidative stress and genomic modification of thymidine induced by ROS following the attachment of a formyl group (45, 47, 48). This chemical modification is relevant for stabilizing 5-FdU binding to MR1 through a Schiff base with the residue Lys 43 in the MR1 A' pocket. However, it is insufficient to make this molecule antigenic, as 5-FU, which similarly makes a Schiff base but lacks the ribose moiety, is not stimulatory. The structural analysis of the MR1-5-FdU complex revealed that the ribose is orientated toward the narrow outer side of the A'-pocket in a position that might interact with TCR residues. Ribose protrudes from the pocket in a direction opposite to that of the ribityl moiety of 5-OP-RU and may be a reason for the lack of MAIT stimulation.

The identification of the 5-FdU antigen and the use of MR1-5-FdU tetramers allowed the characterization of MR1T cells with this Ag specificity. These cells are present in healthy donors with variable frequency, can be $CD4^+$, $CD8^+$, or DN phenotype, and express markers of naïve-, memory-, and effector-memory-like cells. In some donors, the naïve population predominates, which may indicate the presence of cells capable of binding

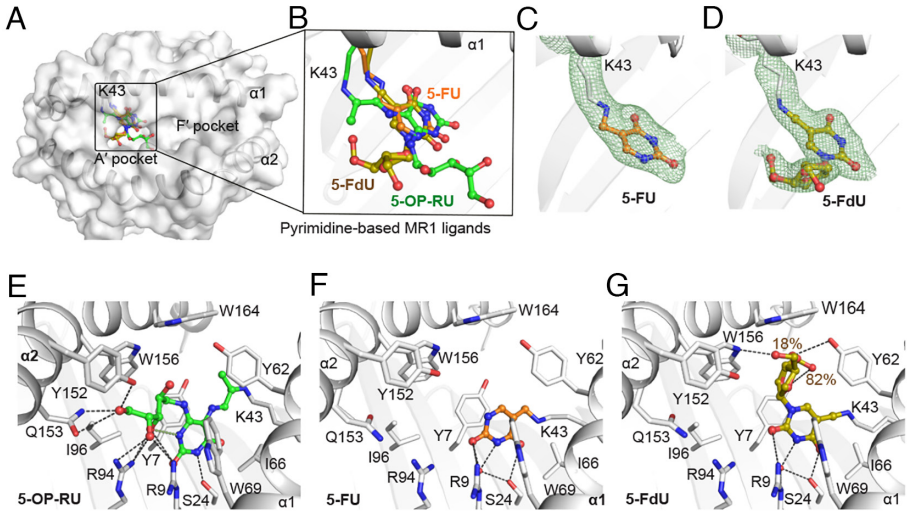

Fig. 7. Crystal structures of MR1 complexed with 5FU and 5-FdU. (*A*) *Top* view of the antigen binding cleft of the respective MR1 molecules displaying the position of the 5-FU and 5F-dU within the A' pocket of MR1. (*B*) Zoomed view of the A' pocket revealing novel orientation of the deoxyribose sugar of 5-FdU compared to the ribityl chain of 5-OP-RU. (*C* and *D*) Electron density maps of 5-FU (*C*) and 5-FdU (*D*) after simulated-annealing refinement (using the Phenix-refine crystallographic structure-refinement program), presented as a $2F_{observed}–F_{calculated}$ map (green mesh) contoured at 1σ that highlight the unambiguous positions of the nucleobases within MR1 cleft. (*E–G*) Interactions between the 5-OP-RU (PDB; 6PUC) (*E*), 5-FU (*F*), and 5-FdU (*G*) and the residues of MR1- A' pocket. MR1 is white, and the ligands are as follows: 5-FU, orange; 5-FdU, olive; and 5-OP-RU, green. The CDR3α and CDR3β loop are pink and light blue, respectively. See also *SI Appendix*, Fig. S8 and Table S1.

to the MR1-5FdU tetramer that are not antigen-experienced. Future studies will address whether MR1-5-FdU-reactive T cells change their phenotype and are increased in patients with different diseases.

These findings indicate that MR1T cells recognizing mitochondria-derived antigens resemble other adaptive-like T cells. Our studies also showed that most MR1-5-FdU tetP T cells do not react with MR1 tetramers presenting the MAIT antigen 5-OP-RU, aligning with the structural data. Only a few cells are stained with MR1-Ac-6-FP tetramers, indicating the presence of a few cross-reactive TCRs. Thus, most of the 5-FdU-reactive TCRs remain specific when challenged with another antigen buried deep within the MR1 cleft and do not react to MR1 loaded with whatever antigen.

An interesting issue is whether cancer cells, which undergo a metabolic switch from OXPHOS to glycolysis, still produce carbonyl adducts of nucleobases and stimulate MR1T cells. This is the case, as cells under high glycolysis conditions accumulate carbonyls such as methylglyoxal (57). This toxic metabolite induces carbonyl stress (58), promotes inflammation and oxidative stress (59), and causes DNA damage (60). Methylglyoxal is significant in generating a group of self (26) and bacterial (20) carbonyl adducts. This evidence indicates that cells utilizing a high glycolytic pathway can also produce carbonyl adducts of nucleobases.

In conclusion, these studies identify the mechanisms involved in the role of mitochondria in the immune response of MR1-restricted T cells. Supplying endogenous metabolites, mitochondria maintain physiological MR1 levels on the plasma membrane and assist in generating T cell antigenic metabolites. These functions give the immune system additional mechanisms to survey metabolically altered cells. While protein synthesis and peptide generation enable classical T cell immunity to recognize immunogenic peptides presented by MHC molecules, mitochondria support the immune response to cells with altered pyrimidine synthesis and ROS accumulation. These changes generate unique metabolites that bind to MR1 and stimulate specific T cells. The physiological implications of this antigen-specific recognition will underlie future studies conducted in patients with various diseases.

Materials and Methods

Human Samples and Study Approval. Human blood samples from healthy donors were obtained from the University Hospital Basel. The study was approved by the local ethical review board (EKNZ, Ethics Committee North-West & Central Switzerland, EKNZ 2017-01888), and all donors consented in writing to analyze their samples.

Human Cell Lines and T Cell Clones. The following human cell lines were initially obtained from the American Type Culture Collection, A375 (melanoma, CRL-1619), and THP-1 (myelomonocytic leukemia, TIB-202) or from the European Collection of Authenticated Cell Cultures, RPMI-7932 (melanoma, CVCL_2713) or kindly donated by Giulio Spagnoli Mel JuSo (melanoma, CVCL_1403). The HEK 293T cell line was obtained from the Leibniz-Institute DSMZ-German Collection of Microorganisms and Cell Cultures. A375 β2m-KO cells overexpressing human MR1 (UniProt Q95460-1) linked to β2m (A375-MR1) are described in ref. 24. THP-1 cells overexpressing human CD1a, CD1b, CD1c, and CD1d were previously generated (61). J.RT3-T3.5 were engineered to lack endogenous TCRα protein and express an NFAT-driven luciferase reporter (27). All cells were routinely tested for the absence of *Mycoplasma* contamination by PCR analysis on DNA samples. None of the cell lines used in this study are in the database of commonly misidentified cell lines. Cell lines were not authenticated. All cells were cultured in RPMI-1640 supplemented with 10% FCS, 2 mM L-glutamine, 1 mM sodium pyruvate, 1x MEM NEAA, and 50 μg/mL kanamycin (complete medium) (all from Bioconcept) unless otherwise indicated. The human MAIT clone MRC25 (ref. 62) and the MR1T cell clones AC1A4, AC1B76, CHO9A4, DGB70, DGB129, LMC1D1, MCA3C3, QY1A16, TC5A87, TRA44 were previously generated and described (24, 26). GP03B5, GP10B5, GP2A20, and GP2A36 clones were generated in this study from the blood of various healthy donors. T cell clones were cultured in RPMI-1640 supplemented with 5% AB-positive human serum (Blutspendezentrum Basel), 2 mM L-glutamine, 1 mM sodium pyruvate, 1× MEM NEAA, and 50 μg/mL kanamycin (complete medium) (all from Bioconcept) and 100 U/mL recombinant human IL-2 (Peprotech).

Evaluation of Mitochondrial Activity and ROS Production. To evaluate mitochondrial potential, mitochondrial mass, and ROS production, cells were stained with MitoTracker Red (200 nM, Thermo Fisher, Cat#M7512), NAO (400 nM, Sigma Aldrich, Cat#A7847), and H_2DCFDA (Thermo Fisher 4 mM, Cat#D399). The staining was performed in complete media for 20 min at 37 °C. The cells were then washed in PBS before analysis. Samples were analyzed on CytoFLEX with CytExpert software (Beckman Coulter). Doublets and dead cells were excluded based on forward scatter area (FSC-A) and forward scatter height (FSC-H, for doublets exclusion) and on forward scatter-width (FSC-W) and staining with DAPI (Sigma, Cat#MBD0015) (for dead cells exclusion).

Generation and Validation of ρ^0 Cells. Mitochondrial DNA was depleted from A375-MR1 cells, as described (63). Briefly, cells were treated with ethidium bromide (1 μg/mL, Sigma-Aldrich, Cat#E1510) and 2′,3′-dideoxy-cytidine (50 μg/mL, Sigma-Aldrich, Cat#D5782) in the presence of uridine (50 μg/mL, Sigma-Aldrich, Cat#U3003). After 4 wk of incubation, cells were tested for the presence of the ND-1 and ND-5 mitochondrial genes by PCR. ND1-, ND5-, and GAPDH-specific primer pairs were used in PCRs with GoTaq G2 DNA polymerase (Promega, Cat#M7845). Clones were generated by limiting dilution and expansion. PCR confirmed the lack of mitochondrial genes.

Refolding and Purification of MR1 and MAIT TCR. Human A-F7 (TRAV1-2/TRBV6-1) MAIT TCR proteins were refolded from inclusion bodies at 4 °C overnight in the refolding buffer containing 0.1 M Tris pH 8.5, 6 M urea, 2 mM EDTA, 0.4 M L-arginine, 0.5 mM oxidized glutathione and 5 mM reduced glutathione as described (29). The wild-type MR1-β2m was refolded in the same refolded buffer, along with the 10× molar ratio of the investigated compound as described previously (20). Refolded MR1-ligand and TCR proteins were purified by three sequential purification steps: crude DEAE anion exchange, S200 15/60 size exclusion chromatography, and HiTrap-Q HP anion exchange. The protein quality and purity were then assessed using sodium dodecyl sulfate-polyacrylamide gel electrophoresis (SDS-PAGE), concentrated, and further quantified using a NanoDrop™ UV-Vis spectrophotometer.

Crystallization, Data Collection, Structure Determination, and Refinement. Purified A-F7 (TRAV1-2/TRBV6-1) TCR was mixed with MR1-β2m-Ag in a 1:1 molar ratio at 4 to 6 mg/mL concentration and kept on ice for 2 h. Hanging-drop, vapor diffusion method at 20 °C was utilized to produce A-F7 TCR-MR1-Ag crystals with a precipitant reservoir solution consisting of 100 mM Bis–Tris Propane (BTP; pH 6.0 to 6.7), 10 to 20% PEG3350 and 200 mM sodium acetate, as reported previously (20). The ternary complexes crystals were grown after a week and harvested, quickly soaked in reservoir solution with 10 to 14% glycerol for cryoprotection, and then flash-frozen in liquid nitrogen. X-ray diffraction datasets were collected at 100 K on the Australian Synchrotron at MX1 or MX2 beamlines. Diffraction data were processed using XDS (64) and programs from the CCP4 suite (65) and Phenix package (66). The previously solved A-F7 TCR and MR1 structures (PDB, 6PUC) (41) were used as a search model for molecular replacement in the PHASER program (67) to solve the ternary structure of TCR-MR1-Ags complexes. The Grade Webserver and Phenix tools were used to build and generate ligand restraints. Model building in COOT (68) was followed by iterative rounds of refinement using Phenix.refine (66), and the models were validated using MolProbity (69). The final refinement statistics of the panel of TCR-MR1-nucleotides are summarized in *SI Appendix*, Table S1. The contacts generated by the Contact program form the CCP4 suite (65). Molecular graphics representations were generated using PyMOL Molecular Graphics System, Version 2.2 (Schrödinger, LLC, New York, NY).

Statistical Analysis. The appropriate statistical test is indicated in the Figure legends and performed using Prism 9 GraphPad software. A P-value < 0.05 was considered statistically significant.

Data, Materials, and Software Availability. The accession number for the atomic coordinates of A-F7 TCR–MR1 in complex with 5-FU and 5-FdU, along with associated structure factors, have been deposited at the protein databank (www.rcsb.org) with accession codes 9EK6 (70) and 9EK7 (71), respectively. All other data are included in the manuscript and/or *SI Appendix*.

ACKNOWLEDGMENTS. We thank Christian Frezza, José Antonio Enriquez, and Marco Lepore for critically reviewing the manuscript, Giulia Montanelli for contributing to experiments, and Feng Zhang for Addgene plasmids 52962 and 52963. The MR1 tetramer technology was developed jointly by Dr. James McCluskey, Dr. Jamie Rossjohn, and Dr. David Fairlie. MR1-5-OP-RU and MR1-6-FP tetramers were produced by the NIH Tetramer Core Facility as permitted to be distributed by the University of Melbourne. This work was supported by grants from the Swiss NSF (310030-173240 and 310030B-192828), Swiss Cancer Research Foundation (KFS-4707-02-2019), Cancer League beider Basel (KLbB-4779-02-2019) to G.D.L. We thank the staff at the Monash Macromolecular Crystallization Facility and the Melbourne Cytometry Platform (Doherty Institute node) for expert assistance. This research used the MX2 beamline at the Australian Synchrotron, part of Australian Nuclear Science and Technology Organisation, and used the Australian Cancer Research Foundation detector. This work was supported by the NIH RO1 AI148407-01A1. W.A. is supported by an Australian Research Council Discovery Early Career Researcher Award (DE220101491). An Australian National Health and Medical Research Council Investigator Award and ARC Discovery grant support J.R.

Author affiliations: [a]Experimental Immunology, Department of Biomedicine, University Hospital Basel, University of Basel, Basel 4031, Switzerland; [b]Infection and Immunity Program and Department of Biochemistry and Molecular Biology, Biomedicine Discovery Institute, Monash University, Clayton, VIC 3800, Australia; and [c]Institute of Infection and Immunity, School of Medicine, Cardiff University, Cardiff CF14 4YS, United Kingdom

Author contributions: G.P. and G.D.L. designed research; G.P., G.B., W.A., A.V., A.C., V.S., D.C., D.R.L., R.C., and V.N. performed research; G.B. and V.S. contributed new reagents/analytic tools; G.P., G.B., W.A., A.V., A.C., V.S., D.C., R.C., V.N., L.M., and J.R. analyzed data; W.A., J.R. and G.D.L. funding recipients; and G.P., G.B., L.M., J.R., and G.D.L. wrote the paper.

Competing interest statement: A.V., A.C., L.M., and G.D.L. are inventors on patent applications submitted by the University of Basel covering the use of MR1T cells and nucleobase adducts for immunomodulation. J.R. is an inventor on patents describing MR1 ligands and MR1 tetramers. All other authors declare no competing interests.

1. A. S. Monzel, J. A. Enriquez, M. Picard, Multifaceted mitochondria: Moving mitochondrial science beyond function and dysfunction. *Nat. Metab.* **5**, 546–562 (2023).
2. R. Z. Zhao, S. Jiang, L. Zhang, Z. B. Yu, Mitochondrial electron transport chain, ROS generation and uncoupling (Review). *Int. J. Mol. Med.* **44**, 3–15 (2019).
3. A. J. Anderson, T. D. Jackson, D. A. Stroud, D. Stojanovski, Mitochondria-hubs for regulating cellular biochemistry: Emerging concepts and networks. *Open Biol.* **9**, 190126 (2019).
4. A. Angajala *et al.*, Diverse roles of mitochondria in immune responses: Novel insights into immuno-metabolism. *Front. Immunol.* **9**, 1605 (2018).
5. A. Bahat, T. MacVicar, T. Langer, Metabolism and innate immunity meet at the mitochondria. *Front. Cell Dev. Biol.* **9**, 720490 (2021).
6. M. R. Mamedov *et al.*, CRISPR screens decode cancer cell pathways that trigger gammadelta T cell detection. *Nature* **621**, 188–195 (2023).
7. K. C. Mangalhara *et al.*, Manipulating mitochondrial electron flow enhances tumor immunogenicity. *Science* **381**, 1316–1323 (2023).
8. T. Sasada, Y. Ghendler, J. M. Neveu, W. S. Lane, E. L. Reinherz, A naturally processed mitochondrial self-peptide in complex with thymic MHC molecules functions as a selecting ligand for a viral-specific T cell receptor. *J. Exp. Med.* **194**, 883–892 (2001).
9. S. Pierini *et al.*, A tumor mitochondria vaccine protects against experimental renal cell carcinoma. *J. Immunol.* **195**, 4020–4027 (2015).
10. G. Prota *et al.*, Enhanced immunogenicity of mitochondrial-localized proteins in cancer cells. *Cancer Immunol. Res.* **8**, 685–697 (2020).
11. G. Prota, A. V. Lechuga-Vieco, G. De Libero, Mitochondrial proteins as source of cancer neoantigens. *Int. J. Mol. Sci.* **23**, 2627 (2022).
12. K. S. Voo *et al.*, CD4+ T-cell response to mitochondrial cytochrome B in human melanoma. *Cancer Res.* **66**, 5919–5926 (2006).
13. D. Cox *et al.*, Determination of cellular lipids bound to human CD1d molecules. *PLoS One* **4**, e5325 (2009).
14. M. Dieude *et al.*, Cardiolipin binds to CD1d and stimulates CD1d-restricted gammadelta T cells in the normal murine repertoire. *J. Immunol.* **186**, 4771–4781 (2011).
15. F. Facciotti *et al.*, Peroxisome-derived lipids are self antigens that stimulate invariant natural killer T cells in the thymus. *Nat. Immunol.* **13**, 474–480 (2012).
16. A. Shahine *et al.*, A molecular basis of human T cell receptor autoreactivity toward self-phospholipids. *Sci. Immunol.* **2**, eaao1384 (2017).
17. H. Li *et al.*, Integrated proteomic and metabolomic analyses of the mitochondrial neurodegenerative disease MELAS. *Mol. Omics* **18**, 196–205 (2022).
18. I. Aretz, C. Hardt, I. Wittig, D. Meierhofer, An impaired respiratory electron chain triggers down-regulation of the energy metabolism and de-ubiquitination of solute carrier amino acid transporters. *Mol. Cell Proteomics* **15**, 1526–1538 (2016).
19. L. Kjer-Nielsen *et al.*, MR1 presents microbial vitamin B metabolites to MAIT cells. *Nature* **491**, 717–723 (2012).
20. A. J. Corbett *et al.*, T-cell activation by transitory neo-antigens derived from distinct microbial pathways. *Nature* **509**, 361–365 (2014).
21. N. A. Gherardin *et al.*, Diversity of T cells restricted by the MHC class I-related molecule MR1 facilitates differential antigen recognition. *Immunity* **44**, 32–45 (2016).
22. A. N. Keller *et al.*, Drugs and drug-like molecules can modulate the function of mucosal-associated invariant T cells. *Nat. Immunol.* **18**, 402–411 (2017).
23. M. Salio *et al.*, Ligand-dependent downregulation of MR1 cell surface expression. *Proc. Natl. Acad. Sci. U.S.A.* **117**, 10465–10475 (2020).
24. M. Lepore *et al.*, Functionally diverse human T cells recognize non-microbial antigens presented by MR1. *Elife* **6**, e24476 (2017).
25. E. Ito *et al.*, Sulfated bile acid is a host-derived ligand for MAIT cells. *Sci. Immunol.* **9**, eade6924 (2024).
26. A. Vacchini *et al.*, Nucleobase adducts bind MR1 and stimulate MR1-restricted T cells. *Sci. Immunol.* **9**, eadn0126 (2024).
27. A. Chancellor *et al.*, Promiscuous recognition of MR1 drives self-reactive mucosal-associated invariant T cell responses. *J. Exp. Med.* **220**, e20221939 (2023).
28. J. Symersky, D. Osowski, D. E. Walters, D. M. Mueller, Oligomycin frames a common drug-binding site in the ATP synthase. *Proc. Natl. Acad. Sci. U.S.A.* **109**, 13961–13965 (2012).
29. S. B. Eckle *et al.*, A molecular basis underpinning the T cell receptor heterogeneity of mucosal-associated invariant T cells. *J. Exp. Med.* **211**, 1585–1600 (2014).
30. M. P. King, G. Attardi, Human cells lacking mtDNA: Repopulation with exogenous mitochondria by complementation. *Science* **246**, 500–503 (1989).
31. S. Guerrero-Castillo, J. van Strien, U. Brandt, S. Arnold, Ablation of mitochondrial DNA results in widespread remodeling of the mitochondrial complexome. *EMBO J.* **40**, e108648 (2021).
32. A. Alexandre, A. L. Lehninger, Bypasses of the antimycin a block of mitochondrial electron transport in relation to ubisemiquinone function. *Biochim. Biophys. Acta* **767**, 120–129 (1984).
33. D. Kampjut, L. A. Sazanov, The coupling mechanism of mammalian respiratory complex I. *Science* **370**, eabc4209 (2020).
34. G. A. Hakkaart, E. P. Dassa, H. T. Jacobs, P. Rustin, Allotopic expression of a mitochondrial alternative oxidase confers cyanide resistance to human cell respiration. *EMBO Rep.* **7**, 341–345 (2006).
35. E. Perales-Clemente *et al.*, Restoration of electron transport without proton pumping in mammalian mitochondria. *Proc. Natl. Acad. Sci. U.S.A.* **105**, 18735–18739 (2008).
36. K. Matsukawa, T. Kamata, K. Ito, Functional expression of plant alternative oxidase decreases antimycin A-induced reactive oxygen species production in human cells. *FEBS Lett.* **583**, 148–152 (2009).
37. S. Boukalova *et al.*, Dihydroorotate dehydrogenase in oxidative phosphorylation and cancer. *Biochim. Biophys. Acta Mol. Basis Dis.* **1866**, 165759 (2020).
38. H. E. McWilliam *et al.*, The intracellular pathway for the presentation of vitamin B-related antigens by the antigen-presenting molecule MR1. *Nat. Immunol.* **17**, 531–537 (2016).
39. M. Fiorillo *et al.*, Repurposing atovaquone: Targeting mitochondrial complex III and OXPHOS to eradicate cancer stem cells. *Oncotarget* **7**, 34084–34099 (2016).
40. M. E. Jones, Pyrimidine nucleotide biosynthesis in animals: Genes, enzymes, and regulation of UMP biosynthesis. *Annu. Rev. Biochem.* **49**, 253–279 (1980).
41. W. Awad *et al.*, The molecular basis underpinning the potency and specificity of MAIT cell antigens. *Nat. Immunol.* **21**, 400–411 (2020).
42. S. F. Chen, R. L. Ruben, D. L. Dexter, Mechanism of action of the novel anticancer agent 6-fluoro-2-(2′-fluoro-1,1′-biphenyl-4-yl)-3-methyl-4-quinolinecarbo xylic acid sodium salt (NSC 368390): Inhibition of de novo pyrimidine nucleotide biosynthesis. *Cancer Res.* **46**, 5014–5019 (1986).
43. M. S. Cooke, M. D. Evans, M. Dizdaroglu, J. Lunec, Oxidative DNA damage: Mechanisms, mutation, and disease. *FASEB J.* **17**, 1195–1214 (2003).
44. A. Y. Andreyev, Y. E. Kushnareva, A. N. Murphy, A. A. Starkov, Mitochondrial ROS metabolism: 10 years later. *Biochemistry (Mosc)* **80**, 517–531 (2015).
45. L. S. Runtsch, M. Stadlmeier, A. Schon, M. Muller, T. Carell, Comparative nucleosomal reactivity of 5-formyl-uridine and 5-formyl-cytidine. *Chemistry* **27**, 12747–12752 (2021).
46. J. Alexandre *et al.*, Accumulation of hydrogen peroxide is an early and crucial step for paclitaxel-induced cancer cell death both in vitro and in vivo. *Int. J. Cancer* **119**, 41–48 (2006).
47. Y. Yu *et al.*, Ultrasensitive simultaneous detection of multiple rare modified nucleosides as promising biomarkers in low-put breast cancer DNA samples for clinical multi-dimensional diagnosis. *Molecules* **27**, 7041 (2022).
48. H. P. Jiang *et al.*, Determination of formylated DNA and RNA by chemical labeling combined with mass spectrometry analysis. *Anal. Chim. Acta* **981**, 1–10 (2017).
49. L. J. Howson *et al.*, Absence of mucosal-associated invariant T cells in a person with a homozygous point mutation in MR1. *Sci. Immunol.* **5**, eabc9492 (2020).
50. P. A. Wearsch, P. Cresswell, Selective loading of high-affinity peptides onto major histocompatibility complex class I molecules by the tapasin-ERp57 heterodimer. *Nat. Immunol.* **8**, 873–881 (2007).
51. A. Chancellor *et al.*, The carbonyl nucleobase adduct M(3)Ade is a potent antigen for adaptive polyclonal MR1-restricted T cells. *Immunity* **58**, 431–447.e10 (2025), 10.1016/j.immuni.2024.11.019.
52. L. B. Sullivan, N. S. Chandel, Mitochondrial reactive oxygen species and cancer. *Cancer Metab.* **2**, 17 (2014).
53. F. Gentile *et al.*, DNA damage by lipid peroxidation products: Implications in cancer, inflammation and autoimmunity. *AIMS Genet.* **4**, 103–137 (2017).
54. A. Ayala, M. F. Munoz, S. Arguelles, Lipid peroxidation: Production, metabolism, and signaling mechanisms of malondialdehyde and 4-hydroxy-2-nonenal. *Oxid. Med. Cell. Longev.* **2014**, 360438 (2014).
55. R. Nilsson *et al.*, Metabolic enzyme expression highlights a key role for MTHFD2 and the mitochondrial folate pathway in cancer. *Nat. Commun.* **5**, 3128 (2014).
56. D. Pluskota-Karwatka, Modifications of nucleosides by endogenous mutagens-DNA adducts arising from cellular processes. *Bioorg. Chem.* **36**, 198–213 (2008).
57. I. Allaman, M. Belanger, P. J. Magistretti, Methylglyoxal, the dark side of glycolysis. *Front. Neurosci.* **9**, 23 (2015).

58. N. Rabbani, Methylglyoxal and glyoxalase 1–a metabolic stress pathway–linking hyperglycemia to the unfolded protein response and vascular complications of diabetes. *Clin. Sci. (Lond.)* **136**, 819–824 (2022).
59. C. Tikellis *et al.*, Dicarbonyl stress in the absence of hyperglycemia increases endothelial inflammation and atherogenesis similar to that observed in diabetes. *Diabetes* **63**, 3915–3925 (2014).
60. M. Frischmann, C. Bidmon, J. Angerer, M. Pischetsrieder, Identification of DNA adducts of methylglyoxal. *Chem. Res. Toxicol.* **18**, 1586–1592 (2005).
61. F. Facciotti *et al.*, Fine tuning by human CD1e of lipid-specific immune responses. *Proc. Natl. Acad. Sci. U.S.A.* **108**, 14228–14233 (2011).
62. M. Lepore *et al.*, Parallel T-cell cloning and deep sequencing of human MAIT cells reveal stable oligoclonal TCRbeta repertoire. *Nat. Commun.* **5**, 3866 (2014).
63. N. Khozhukhar, D. Spadafora, Y. Rodriguez, M. Alexeyev, Elimination of mitochondrial DNA from mammalian cells. *Curr. Protoc. Cell Biol.* **78**, 20.11.1–20.11.14 (2018).
64. W. Kabsch, Integration, scaling, space-group assignment and post-refinement. *Acta Crystallogr. D Biol. Crystallogr.* **66**, 133–144 (2010).
65. M. D. Winn *et al.*, Overview of the CCP4 suite and current developments. *Acta Crystallogr. D Biol. Crystallogr.* **67**, 235–242 (2011).
66. P. D. Adams *et al.*, PHENIX: A comprehensive Python-based system for macromolecular structure solution. *Acta Crystallogr. D Biol. Crystallogr.* **66**, 213–221 (2010).
67. A. J. McCoy, Solving structures of protein complexes by molecular replacement with Phaser. *Acta Crystallogr. D Biol. Crystallogr.* **63**, 32–41 (2007).
68. P. Emsley, K. Cowtan, Coot: Model-building tools for molecular graphics. *Acta Crystallogr. D Biol. Crystallogr.* **60**, 2126–2132 (2004).
69. V. B. Chen *et al.*, MolProbity: All-atom structure validation for macromolecular crystallography. *Acta Crystallogr. D Biol. Crystallogr.* **66**, 12–21 (2010).
70. W. Awad, J. Rossjohn, Data from "Crystal structure of MAIT TCR in complex with MR1-5FU." Protein Data Bank. https://doi.org/10.2210/pdb9EK6/pdb. Deposited 1 December 2024.
71. W. Awad, J. Rossjohn, Data from "Crystal structure of MAIT TCR in complex with MR1-5FdU." Protein Data Bank. https://doi.org/10.2210/pdb9EK7/pdb. Deposited 1 December 2024.